ACS Catalysis

Research Article

pubs.acs.org/acscatalysis

Thermodynamic Descriptors for Molecules That Catalyze Efficient CO_2 Electroreductions

Aude Marjolin and John A. Keith*

Department of Chemical and Petroleum Engineering, Swanson School of Engineering, University of Pittsburgh, 3700 O'Hara Street, Pittsburgh, Pennsylvania 15261, United States

Supporting Information

ABSTRACT: Guiding proton and electron transfers in an energetically efficient manner remains a hurdle in renewable energy catalysis. To help identify and better understand efficient CO_2 conversion catalysts, we used first-principles quantum chemistry to determine pH and electrode potential dependent energies for different classes of aromatic N-heterocycles based on pyridine and imidazole moieties. From these data, we locate Pourbaix diagram triple points that denote the electrochemical conditions where these molecules would facilitate energetically efficient proton or hydride shuttling. Within surprisingly reasonable accuracy, the calculated molecular Pourbaix diagram triple points correspond to experimental conditions under which molecular-promoted CO_2 reduction has been observed. This indicates a novel thermodynamic descriptor suitable for high-throughput computational screening can be used to predict molecular cocatalysts and their ideal reaction conditions for renewable energy catalysis.

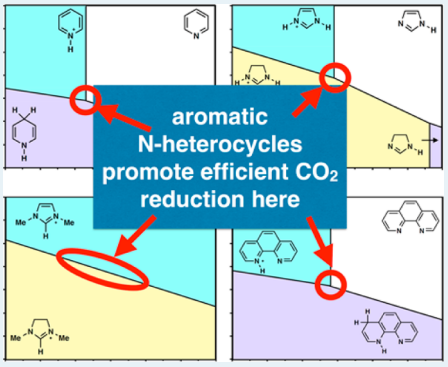

KEYWORDS: *CO_2 reduction, aromatic N-heterocycles, hydride transfer, quantum chemistry calculations, continuum solvation, molecular Pourbaix diagrams, pyridinium, imidazolium*

INTRODUCTION

Discovering and engineering sources of renewable energy are paramount to long-term human sustainability. One route is to generate renewable fuels in a carbon-neutral manner, for example, via solar fuels processes.[1,2] Unfortunately, many fuel-generating processes are impractical as a result of poor conversion efficiencies, high overpotentials, or both. Carrying out proton and electron transfers selectively in an energetically efficient manner remains a significant hurdle for renewable fuels catalysis.

Many CO_2 conversion processes can be driven only with high overpotentials. These can be attributed either to the requisite energy to add an electron to CO_2 to form $CO_2^{\bullet-}$ (−2.14 V vs the saturated calomel electrode, SCE)[3] or to the energy required to remove reaction intermediates (i.e., CO or CHO) that block reaction sites on the catalyst.[4] Because proton-coupled electron transfer (PCET) mechanisms[5−7] are less endoergic, incorporating Brønsted acids in these systems may be expected to lower overpotentials by providing protons for PCET. On the other hand, added protons can also be expected to increase rates for the hydrogen evolution reaction (HER), lowering selectivities for CO_2 reduction products as well as overall efficiencies. Ideally, one must discover processes that do not require high overpotentials but also selectively reduce CO_2 (but not protons).

Different research groups have recently reported CO_2 reduction at remarkably low overpotentials and with high faradic efficiencies. Coincidentally, all these studies used aromatic N-heterocycles (ANHs) in mostly aqueous solutions. Bocarsly and co-workers reported that pyridinium (PyH^+)[8−10] and imidazolium (ImH^+)[11] promote CO_2 reduction to different products on different electrode materials. Masel and co-workers,[12−14] reported low overpotentials and high faradic efficiencies for forming CO in 18 mol % 1-ethyl-3-methyl-imidazolium (EMIM) in water. MacDonnell and co-workers[15] found CO_2 reduction to methanol with PyH^+ in homogeneous photochemical cells with $[Ru(phen = phenanthroline)_3]^{2+}$ chromophores. Dyer et al. demonstrated that mercaptopyridines are involved in CO_2 reduction on glassy carbon electrodes.[16] ANHs are also common moieties in ionic liquids that already have widespread use for CO_2 capture.[17,18] Thus, one might ponder if ANH molecules (e.g. those in Figure 1) share a similar physical property that would indicate that they

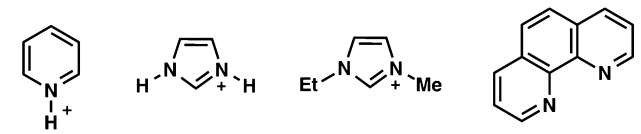

Figure 1. Aromatic N-heterocycles (ANHs) implicated in CO_2 conversion catalysis.

Received: September 16, 2014
Revised: December 8, 2014
Published: January 6, 2015

DOI: 10.1021/cs501406j
ACS Catal. 2015, 5, 1123−1130

all play a similar role in CO_2 reduction. We note that current densities for these processes are fairly low (~10 mA·cm^{-2}), but understanding why ANH molecules might cause lower overpotentials and higher faradic efficiencies would provide helpful design principles for improved renewable energy catalysts.

PYRIDINIUM-PROMOTED CO_2 REDUCTION

The ANH systems receiving the most mechanistic attention have been PyH^+ systems first reported by Bocarsly's group. These have garnered investigations from both theory[19−24] and experiment.[11,25−27] The electrode in these electrochemical systems plays key role that remains not well understood. Interestingly, CO_2 reduction has been reported using cyclic voltammetry (CV) measurements operating at rather low scan rates ranging from 1 to 50 mV·s^{-1}, while Savéant et al. have suggested that natural convection at these scan rates influences voltammetric responses.[25] That group also reported no ANH-promoted CO_2 reduction at higher scan rates (100−200 mV·s^{-1}), thereby raising the question if ANH-promoted CO_2 reduction was even possible.

Indeed, Bocarsly and co-workers had originally proposed that PyH^+ played a dual role facilitating proton and electron transfers that led to CO_2 conversion to methanol.[8,10] By maintaining the electrolyte's pH equal to the pK_a of PyH^+, the ANH at these reaction conditions would facilitate proton shuttling, since at these conditions, the chemical potentials of Py and PyH^+ in solution would be the same (i.e., protons would be equally likely to be found in solution as on PyH^+). Similarly, by maintaining an applied potential close to what was then known as the literature value for the 1e$^-$ redox potential for $PyH^+ + e^- \rightarrow PyH\cdot$ in aqueous solution on Pt electrodes, −0.58 V vs SCE at pH 5.3, the ANH at these reaction conditions appeared to be facilitating individual electron transfers as well. Thus, one can note that the role of the ANH in this catalysis might be described in terms of the Sabatier Principle.

However, this intriguing one-proton, one-electron shuttle hypothesis appeared to be disproven after first-principles quantum chemistry studies reported that the standard redox potential (SRP) for the aqueous phase reaction of $PyH^+ + e^- \rightarrow PyH\cdot$ was far more negative (~−1.4 V) than previously believed.[19,20,24,28] Recent experimental studies by Bélanger and co-workers supported the computational predictions by showing an observed reduction peak for PyH^+ reduction on glassy carbon electrodes occurred at −1.5 V,[26] which is in quite good agreement with corresponding values predicted with theory as well as negative enough that this peak may have been interpreted as being the onset of water electrolysis. On the basis of this concordance between theory and experiment, it is clear that PyH· is unlikely to form in electrochemical cells at moderate applied potentials, although it does not necessarily rule out the possibility of PyH· forming under photoelectrochemical conditions, as discussed by Musgrave et al.[29] Colussi et al. recently demonstrated that photogenerated PyH· species *can* reduce CO_2 in homogeneous solution;[30] however, despite these more recent perspectives, we are not aware of any spectroscopic evidence of PyH· species forming in electrochemical or photoelectrochemical cells.

The 1e$^-$ reduction observed by CV has also since been established by theory[19] and experiment[25,27] as the PyH^+-assisted reduction of protons to the electrode surface; that is, the observed 1e$^-$ reduction is the formation of an overpotential deposited H atom, H_{opd},[31,32] at weakly acidic conditions. Batista and co-workers were the first to propose this mechanism for this chemistry, suggesting that PyH^+ facilitates H_{opd} formation and supplies protons for proton-coupled hydride transfer processes to form CO_2 reduction products (with the concomitantly transferred H_{opd}).

Although this mechanism had appeared to be the most consistent with experimental observations made thus far, it has at least one significant limitation. It suggests that PyH^+ only transfers protons, leaving the electrode surface to be responsible for transferring the remaining electrons (or protons and electrons in the form of hydrides, H$^-$). If this mechanism were true, any Brønsted acid in this electrochemical environment should carry out a similar role as an PyH^+, but not all Brønsted acids do. First, H_2O is a Brønsted acid, but alone, it does not facilitate this chemistry. Furthermore, Portenkirchner and co-workers have recently reported detecting methanol from CO_2 reduction with PyH^+, but no evidence of methanol from CO_2 reduction with acetic acid, a weak acid with a pK_a similar to that of PyH^+ in otherwise similar conditions.[33] On the basis of these observations, ANH appears to play a key role in CO_2 reduction; however, we reiterate that experimental ANH-promoted CO_2 reduction seems to be highly dependent on the experimental conditions employed as well as the method in which the CO_2 reduction is quantified.

One could also consider if a similar proposed mechanism might be applicable in the other ANH-promoted examples, as well. If the main role of the ANH were to shuttle protons, one might wonder how EMIM molecules with no immediately labile protons (the pK_a of the C_2 proton in imidazolium is ~24) could then catalyze CO_2 reduction to CO under otherwise comparable electrochemical conditions on Ag electrodes.[12−14] In addition, if proton reduction on the electrode surface were, indeed, a key step for these electrochemical processes, one may ask the question how photochemical experiments with no electrode surface would facilitate CO_2 reduction, as demonstrated in studies by MacDonnell and co-workers.[15,34] This is the current state of the puzzle. To unravel this puzzle, we believe it would be useful to understand if these different ANH molecules share any similar characteristics that might allow them to reduce CO_2 efficiently in a similar manner.

We posit that the key role of the ANH molecules in these cases is to efficiently shuttle hydrides to CO_2. Governed by the Sabatier Principle, ANHs would be able to do this only under very specific ambient electrochemical conditions. If the ANH is also a Brønsted acid in the appropriate chemical environment, it may also shuttle protons. The dihydropyridine (DHP) mechanism proposed by Keith and Carter[23] is a hypothetical scenario in which Py/PyH^+ species in Bocarsly's systems might facilitate both proton and hydride shuttling under specific electrochemical conditions. Under the electrochemical conditions similar to those used for CO_2 reduction, quantum chemistry calculations have shown that it is thermodynamically feasible for DHP to exist in solution.[22] (Note that kinetic barriers to form DHP have not yet been established on different electrode surfaces, but Musgrave et al. report reasonable calculated barriers for DHP formation in solution, assuming that PyH· is formed first.[29]) We note that the reaction mechanism by which DHP might form on an electrode surface is unclear; however, a reasonable hypothesis might involve a H_{opd} species from the surface concomitantly transferring with a proton from the electrolyte to a surface-bound Py. It is also promising that DHP moieties are known to be abundant in biological and biomimetic hydride transfer studies as the

DOI: 10.1021/cs501406j
ACS Catal. 2015, 5, 1123−1130

cofactor in NADH and in Hantzsch's ester.[35] However, if DHP actually were formed as an intermediate in these systems, experiments should be able to detect its existence on Pt electrodes. In fact, there has been no experimental evidence of DHP forming or evidence of a 2 e^- transfer processes occurring,[27] leaving this chemistry both intriguing and equally puzzling.

To better understand the fundamental thermodynamic energies of these electrochemical processes, we used first-principles quantum chemistry to determine electrochemical reactivities of different ANHs, shown in Figure 1. Our objective was to identify trends in different ANH molecules to see if those trends provide a clue why different ANH molecules might have been implicated in the CO_2 reductions. We found that all these ANH molecules share a similar feature: namely, a $2e^-$ SRP (accompanied by protons transfers) that is similar to the multielectron SRPs that would reduce CO_2 to various products. As discussed below, this may have very important implications for the development of renewable energy catalysts.

COMPUTATIONAL METHODS

Molecular geometries for all species were carried out using GAMESS-US.[36,37] Pyridine and imidazolium-based molecules were optimized using the B3LYP[38,39]/AVDZ[40] level of theory. Solvation energies (ΔG_s) for molecules in water were calculated using the conductor-based polarization continuum method (CPCM)[41] with cavities defined by the simplified united atom Hartree−Fock (SUAHF) model as implemented in GAMESS-US. Molecules with a Brønsted acid site were treated with an explicit/continuum solvation approach that was shown to improve accuracies of pK_as for substituted pyridinium molecules to errors within 1 pK_a unit.[21] More-accurate electronic energies were then carried out using CCSD(T)-F12b[42]/AVDZ[43−45] calculations with the MOLPRO[46] code, using appropriate basis sets for each calculation component. For larger phenanthroline molecules, geometry optimizations and vibrational frequency calculations were carried out using the smaller 6-31+G* basis set, and single-point electronic energies (and solvation energies) were obtained with B3LYP/AVDZ (and CPCM) to be consistent with other B3LYP data. CCSD(T)-F12/AVDZ calculations were not carried out for phenanthroline molecules; however, we found in comparison with pyridinium and imidazolium cases, pK_as, hydricities, and SRPs from B3LYP/AVDZ are comparable to those using CCSD(T)-F12/AVDZ. The values calculated by the two different methods differ by less than 1.2 pK_a units: 0.25 eV and 0.15 V, respectively.

This study employed several different established calculation schemes to obtain pK_as,[47] hydricities,[48] and SRPs[49] that are summarized in Scheme 1. In these calculations, $G(H^+_{(g)})$ was taken as −6.3 kcal/mol from the Sackur−Tetrode equation,[50] and $\Delta G_s(H^+)$ was taken as −264.0 kcal/mol (including the free energy contribution needed for the aqueous proton to have a standard state of 1 M).[51] The free energy of an electron at 0 V vs SHE, $G(e^-)$, was taken from the absolute potential of the SHE (−4.28 V) in water[52] and adjusted by −0.24 V so that it corresponded to the absolute potential of the SCE electrode. An in-depth overview of empirically and computationally derived proton and absolute electrode potentials is presented in a recent perspective by Marenich et al.[53] The free energy contribution of an applied electrode potential (ϕ) on a free electron can be incorporated into the calculation scheme by subtracting F (Faraday's constant) × ϕ from the energy of the free electron in any electrochemical reaction step. Finally, for hydricity calculations, the absolute energy of an aqueous phase hydride, H^-, was defined as the gas phase energy of H_2 minus the absolute energy of an aqueous phase proton (−270.3 kcal/mol; see above) plus the energy for H_2 heterolysis in aqueous solution, $\Delta G_{hetero}(H_2)$. There are several different derivations of this value; however, when we use the value employed by Creutz and Muckerman, $\Delta G_{hetero}(H_2)$ = +42.1 kcal/mol,[48] our computationally predicted hydricities of formate with our computational scheme were within 1 kcal/mol (0.05 eV) of the experimental value reported by Creutz and Chou.[54]

Scheme 1. Thermochemical Cycle and Expressions Used To Calculate Electrochemical Energies

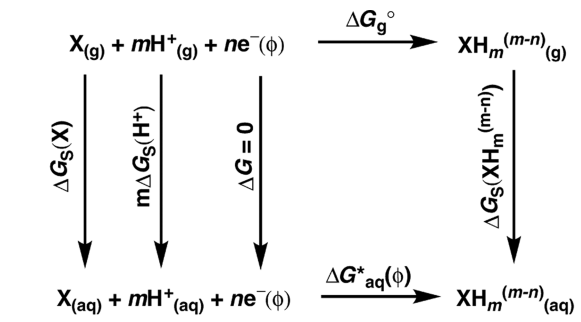

$$\Delta G^*_{aq}(pH,\phi) = G(XH_m^{(m-n)}{}_{(g)}) + \Delta G_S(XH_m^{(m-n)}) - G(X_{(g)}) - \Delta G_S(X) - m\,[G(H^+_{(g)}) - \Delta G_S(H^+) - \ln(10)\cdot RT\cdot pH] - n\,[G(e^-) - F\cdot\phi]$$

For $m = 1$, $n = 0$:

$$\Delta G^*_{aq} = G(XH_m^{(m-n)}{}_{(g)}) + \Delta G_S(XH_m^{(m-n)}) - G(X_{(g)}) - \Delta G_S(X) - G(H^+_{(g)}) - \Delta G_S(H^+)$$

$$pK_a = \frac{-\Delta G^*_{aq}}{\ln(10)\cdot RT}$$

For $m = 1$, $n = 2$:

$$G(H^-) = \Delta G_{hetero}(H_2) + G(H_{2(g)}) - G(H^+_{(g)}) - \Delta G_S(H^+) - \ln(10)\cdot RT\cdot pH$$

$$\Delta G_{hyd}(pH) = G(XH^+_{(g)}) + \Delta G_S(XH^+) + G(H^-) - G(XH_{2(g)}) - \Delta G_S(XH_2)$$

For $m > 0$, $n \geq 0$:

$$E^\circ = \frac{-\Delta G^*_{aq}(pH,\phi)}{n\cdot F}$$

RESULTS AND DISCUSSION

Clearly, ANH-catalyzed CO_2 conversion processes require more investigation to better understand why ANHs might facilitate energetically efficient and selective reduction of CO_2. Understanding this role may also provide design principles for other forms of renewable fuel generation. The success and broad applicability of Nørskov and co-workers' first-principles electrochemical modeling has shown that one needs not know the exact mechanism of an electrochemical process to obtain useful, computationally derived thermodynamic descriptors. By determining the binding energies of a limited number of

DOI: 10.1021/cs501406j
ACS Catal. 2015, 5, 1123−1130

adsorbates on a surface from quantum chemistry, new catalysts can be predicted and then developed with similar or improved performance for hydrogen evolution,[55] oxygen reduction,[56] water oxidation,[57] and CO_2 reduction.[58]

In a similar spirit, we considered the feasibility of a proton/electron shuttling model directly analogous to Bocarsly's original proposal but more general in that it considers species resulting after multiple proton and electron transfers involving different ANH molecules (Figure 2). Calculated data used for this model are tabulated in Table 1. From our calculated data, we also generated molecular Pourbaix diagrams (Figure 3) for the different ANH molecules by considering the relative energies of molecules that differ by the numbers of transferred protons and electrons (using $\Delta G^*_{aq}(\mathrm{pH},\phi)$ values as calculated by Scheme 1). Note that vertical isobars in a Pourbaix diagram correspond to pK_as of the protonated species. Diagonal isobars correspond to (pH-dependent) SRPs for multi-electron and multi-proton transfer processes. The intercepts of these isobars, the Pourbaix diagram triple points, denote electrochemical conditions where thermodynamic energies would be optimal for the ANH species to shuttle both protons and electrons (the latter likely via hydride shuttling).

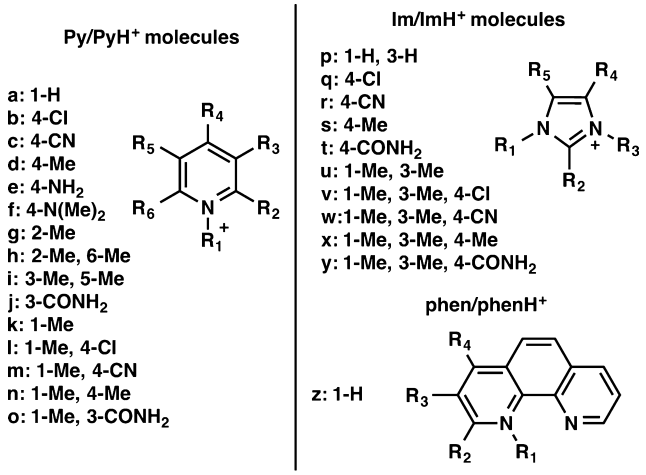

Figure 2. Chemically substituted ANHs considered in this work. Letters are indexes used in Table 1

The molecular Pourbaix diagrams can be interpreted as phase diagrams that show the pH and ϕ at which certain molecular species are energetically stable in solution. Note that the diagrams report solution-phase thermodynamic data and do not account for formation barriers that are electrode-dependent. Nevertheless, these diagrams are a useful starting point for understanding which species are thermodynamically stable at specific electrochemical reaction conditions. On the basis of the accuracy of the quantum chemistry calculations employed, the estimated absolute accuracy of these diagrams on the pH and E scales should be ∼1 pK_a unit and ∼0.20 V, respectively. However, relative differences between different points on the same Pourbaix diagram should be considered to be more accurate.

The Pourbaix diagrams in Figure 3 show a striking similarity among the four different ANH molecules shown in Figure 1. All four molecules have multielectron SRPs (involving protons) in the vicinity of SRPs for proton and CO_2 reduction. *This means that at reduction conditions where protons or CO_2 would be reduced, the ANH molecules themselves may also become reduced.* Even though there has been no experimental evidence of DHP forming in experimental investigations, the 2e$^-$ SRPs for ANHs are similar enough to SRPs for CO_2 reduction that DHP (or other 2e$^-$-reduced species) should be considered as a possible transient intermediate.

In the case of the pyridine Pourbaix diagram, which was reported previously,[22] a triple point lies at the pH equal to the pK_a of PyH$^+$, and the 2e$^-$ SRP to form *p*-DHP varies from −0.64 V at pH 0 to more negative values with increasing pH. The fact that the isobar bordering the purple region in Figure 3a is more negative than the SRPs for CO_2 reduction products indicates that if a *p*-DHP species were to form, there should be a thermodynamic driving force for the reduced ANH to reduce CO_2 to either CO + H_2O or HCO_2^-.

Indeed, this conclusion can also be reached by looking at calculated hydricities reported in Table 1. Donating a hydride from a reduced ANH to CO_2 will be thermodynamically favorable if the hydricity of the reduced ANH is less than ∼1.43 eV (∼33 kcal/mol), the experimental hydricity of formate.[54] Interestingly, the 2e$^-$ SRPs to form *o*-DHP are only slightly more negative than those for *p*-DHP. This means that *p*-DHP would be the thermodynamically more stable intermediate compared with *o*-DHP, but if *o*-DHP also could form, it would be an even stronger hydride donor than *p*-DHP. We note that hydricity discussions invoke only thermodynamics and do not account for barriers for electroreductions. Bocarsly's group reported that DHP mixed with CO_2 and acid does not produce CO_2-reduced products.[27] One possible reason for this is because kinetic barriers for chemical CO_2 reduction in this experiment are high, although electrochemical processes in the presence of an electrode surface may be lower.

Table 1 also shows the extent that different chemical substituents will influence electrochemical reactivities for pyridinium moieties. As expected, adding an electron-withdrawing group (e.g., −Cl or −CN) to the aromatic ring would make DHP species less effective hydride donors and would decrease their 2e$^-$ SRPs. Alternatively, adding electron-donating groups (e.g., −Me) to the aromatic ring increases the hydride-donating ability of the DHP as well as increases the 2e$^-$ SRPs.

Interestingly, adding a Me group to the N1 position of Py has only a minimal effect on the calculated hydricities and 2e$^-$ SRPs. This might suggest that this species would also facilitate hydride shuttling, given the correct electrochemical conditions are used to form the DHP. However, earlier studies by Bocarsly's group found that these *N*-methyl molecules do not participate in CO_2 reduction in electrochemical cells.[10] We speculate this is because *N*-methyl Py molecules will not be able to bind to an electrode surface in sufficient quantities to form its reduced state (which may or may not be DHP-like). Finally, we also considered nicotinamide moieties because they are analogous to cofactors in NAD$^+$/NADH enzymes. We find that the hydricities for these molecules are almost the same as that for formate, indicating that standard nicotinamide molecules are likely not promising avenues to pursue for CO_2 reduction catalysts in these electrochemical environments.

This simple model of the Pourbaix diagram triple point appears to be robust, at least for substituted pyridinium molecules for which there is sufficient experimental data for comparisons. Previous work in the Bocarsly group reported CO_2 reduction could be catalyzed using several different substituted pyridinium molecules,[59] pyridinium as well as 4-Me, 4-NH_2, 4-N(Me)$_2$, 3,5-dimethyl, and 2,6-dimethyl substituted

DOI: 10.1021/cs501406j
ACS Catal. 2015, 5, 1123−1130

Table 1. Calculated Thermodynamic Parameters pK_a's, $E°$ in V vs. SCE, ΔG_{hyd} in eV Calculated in This Study

	entry	substituents	pK_a[a]	pK_a[b]	E^{0c}	ΔG_{hyd}[d]	E^{0e}	ΔG_{hyd}[f]	E^{0g}	E^{0h}
Py/PyH$^+$	a	1-H	4.7 (5.17[t])		−0.71	0.98	−0.64	1.13	−0.50	−0.78
	b	1-H,4-Cl	2.7 (3.83[u])		−0.59	1.22	−0.26	1.88	−0.18	−0.34
	c	1-H,4-CN	1.2 (1.90[v])		−0.46	1.49	−0.41	1.58	−0.37	−0.45
	d	1-H,4-Me	5.5 (6.02[t])		−0.76	0.89	−0.71	0.98	−0.55	−0.88
	e	1-H,4-NH_2	8.9 (9.17[t])	−2.2	−0.93	0.54	−0.93	0.54	−0.67	−1.19
	f	1-H,4-N(Me)$_2$	9.5 (9.7[t])	−2.7	−0.95	0.51	−0.93	0.54	−0.65	−1.21
	g	1-H,2-Me	5.7 (5.94[t])		−0.73	0.94	−0.68	1.05	−0.51	−0.85
	h	1-H,2-Me, 6-Me	6.8 (6.77[t])		−1.27	−0.14	−0.80	0.80	−0.60	−1.01
	i	1-H,3-Me, 5-Me	5.5 (6.14[t])		−0.77	0.87	−0.68	1.05	−0.52	−0.84
	j	1-H,3-$CONH_2$	3.5 (3.4[w])	−7.7	−0.56	1.28	−0.47	1.46	−0.37	−0.58
	k	1-Me, 4-H			−0.71	0.99	−0.67	1.06		
	l	1-Me, 4-Cl			−0.57	1.26	−0.33	1.75		
	m	1-Me, 4-CN			−0.44	1.53	−0.44	1.52		
	n	1-Me, 4-Me			−0.75	0.91	−0.75	0.90		
	o	1-Me, 3-$CONH_2$		−13.3	−0.52	1.36	−0.48	1.44		
	entry	substituents	pK_a[a]	pK_a[b]	pK_a[i]	E^{0j}		ΔG_{hyd}[k]	E^{0l}	E^{0m}
Im/ImH$^+$	p	1,3-H	5.9 (7.05[x])		24.2 (23.8[y])	−0.89		0.72	−0.22	−0.59
	q	1,3-H,4-Cl	2.0		22.1	−0.75		0.91	−0.06	−0.18
	r	1,3-H,4-CN	0.5		22.2	−0.67		1.06	−0.21	−0.24
	s	1,3-H,4-Me	8.0		24.0	−0.97		0.46	−0.26	−0.73
	t	1,3-H,4-$CONH_2$	2.6	−13.4	21.2	−0.87		0.67	−0.22	−0.38
	u	1,3-Me,4-H			22.7 (23.0[y])	−0.94		0.52	−0.22	
	v	1,3-Me,4-Cl			19.9	−0.84		0.73	−0.06	
	w	1,3-Me,4-CN			18.5	−0.73		0.93	−0.21	
	x	1,3-Me,4-Me			23.6	−1.02		0.36	−0.25	
	y	1,3-Me, 4-$CONH_2$		−12.8	20.6	−0.92		0.56	−0.18	
	entry	substituents	pK_a[a]		E^{0m}	ΔG_{hyd}[o]	E^{0p}	ΔG_{hyd}[q]	E^{0r}	E^{0s}
phen/phenH$^+$	z	1-H	5.5 (4.98[z])		−0.60	1.29	−0.55	1.40	−0.38	−0.71

[a]Calculated pK_a at N1 position (experiment, when available). [b]pK_a of protonated substituent (pK_a's for $-CONH_2$ groups are at the O atom). [c]PyH$^+$ + H$^+$ + 2e$^-$ → *o*-DHP, pH 0. [d]Hydricity of *o*-DHP, pH 0. [e]PyH$^+$ + H$^+$ + 2e$^-$ → p-DHP, pH 0. [f]Hydricity of *p*-DHP, pH 0. [g]Py + 2H$^+$ + 2e$^-$ → *p*-DHP, pH 0. [h]Py + 2H$^+$ + 2e$^-$ → *p*-DHP, pH at pK_a from column a. [i]pK_a at C2 position (experiment, when available). [j]ImH$^+$ + H$^+$ + 2e$^-$ → 4-imidazoline, pH 0. [k]Hydricity of 4-imidazoline, pH 0. [l]ImH$^+$ + 2H$^+$ + 2e$^-$ → 2-imidazolinium cation, pH 0. [m]ImH$^+$ + 2H$^+$ + 2e$^-$ → 2-imidazolinium cation, pH = pK_a (a). [m]PhenH$^+$ + H$^+$ + 2e$^-$ → 1,2-DHphen, pH 0. [o]Hydricity of 1,2-DHphen, pH 0. [p]PhenH$^+$ + H$^+$ + 2e$^-$ → 1,4-DHphen, pH 0. [q]Hydricity of 1,4-DHphen, pH 0. [r]Phen +2H$^+$ + 2e$^-$ → 1,4-DHphen, pH 0. [s]Phen +2H$^+$ + 2e$^-$ → 1,4-DHphen, pH = pK_a (from a). [t]Ref 59. [u]Ref 60. [v]Ref 61. [w]Ref 62. [x]Ref 63. [y]Ref 64. [z]Ref 65.

pyridinium molecules. Our calculated pK_as on these species agree with experiment with an average error of 0.3 pK_a units. Furthermore, our calculated 2e$^-$ SRPs for these molecules at pH 5.5 (−0.82, −0.88, −0.99, −0.98, −0.93, and −0.84 V, respectively) are, on average, −0.22 V more negative than the experimental SRPs[59] obtained at pH 5.5 (−0.58, −0.64, −0.79, −0.82, −0.63, and −0.62 V, respectively). We presume that the reported experimental potentials should be attributed to H_{opd} formation with these ANH species, but this signifies that 2e$^-$ SRPs are similar to potentials that would form H_{opd}. Therefore, 2e$^-$ SRPs of ANH molecules should be considered possible in future investigations. Furthermore, quantum chemistry calculations can reasonably predict the pH and ϕ at which pyridine-based ANH molecules would be good proton- or hydride-shuttling agents. The role of the electrode surface remains a question, however. Bélanger and co-workers find that potentials needed for ANH reduction/H_{opd} formation on different surfaces correlate with the HER overpotential for those surfaces.[26]

We now move on to non-N-substituted imidazolium species. The reduced species can accommodate up to three protons from solution and two electrons from the electrode if the starting state is a nonprotonated imidazole. Unlike in the case of pyridinium, there are two triple points that appear under this range of electrochemical conditions. The triple point at the calculated pK_a of imidazolium is less negative than the triple point for the pyridine case, as well as the SRP for CO or HCO_2^-, by ∼0.2 V. This indicates that the 2-imidazoline species would not have the thermodynamic driving force to chemically reduce CO_2, even though experiments have indicated that imidazolium does participate in CO_2 electroreductions.[11]

This disagreement may be due to the fact that our calculated 2e$^-$ SRPs may be, on average, inaccurate by ∼0.2 V. Were these SRPs more negative by 0.2 V, then our proposed hypothesis for 2e$^-$ reduced species' being involved in CO_2 reduction would be supported by experiment. It is also possible that actual surface-bound adsorbate may have a more negative SRP than what we calculate in solution. We also considered the product of a 1H$^+$ + 2e$^-$ reduction of imidazolium that would result in 4-imidazoline, a less stable neutral species with two H atoms on the C_2 carbon. Analogous to the previously described case for *o*-DHP, the 4-imidazoline species is always substantially less stable than imidazole, imidazoline, or 2-imidazoline at all sets of pH and ϕ. However, this would also make it a better hydride donor were it to form. Indeed, with a hydricity of 0.72 eV, 4-imidazoline would be a relatively powerful hydride donor capable of reducing CO_2 with an even larger thermodynamic

DOI: 10.1021/cs501406j
ACS Catal. 2015, 5, 1123−1130

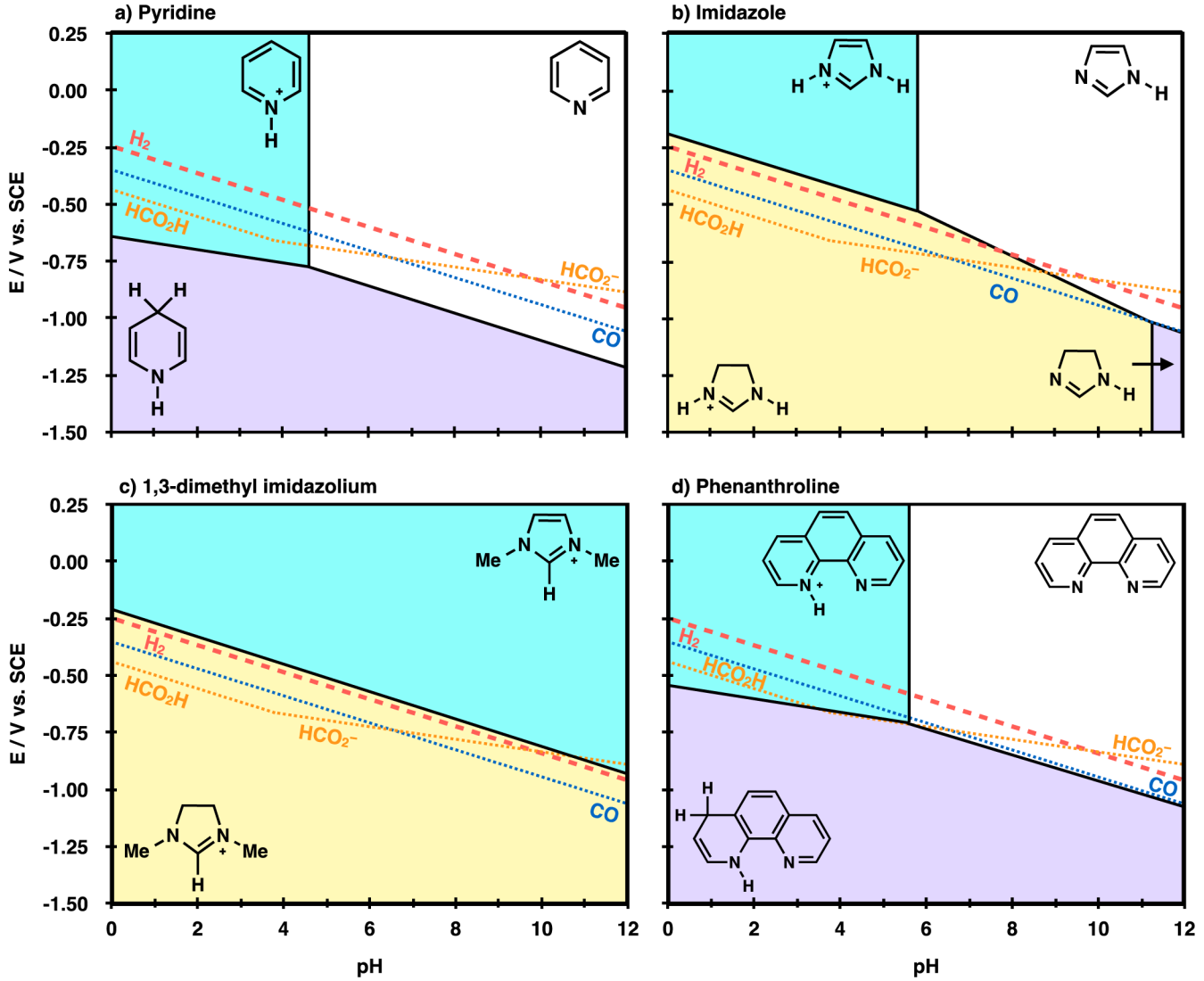

Figure 3. Molecular Pourbaix diagrams for species in Figure 1. The diagrams depict electrochemical conditions (variable pH and E), where nonprotonated (white region), monoprotonated (cyan region), $2H^+ + 2e^-$ reduced (purple region), and $3H^+ + 2e^-$ reduced (yellow region) are the thermodynamically most stable states in water solvent. Overlaid in the diagrams are SRPs for $2H^+ + 2e^- \rightarrow H_2$ (H_2, red dashed line), $CO_2 + 2H^+ + 2e^- \rightarrow CO + H_2O$ (CO, blue dotted line), $CO_2 + 2H^+ + 2e^- \rightarrow HCO_2H$ (HCO_2H) and $CO_2 + H^+ + 2e^- \rightarrow HCO_2^-$ (HCO_2^-, gold dotted lines). At applied potentials, more negative than these lines, product species would be thermodynamically stable compared with reactant protons, electrons, and CO_2.

driving force than either *p*-DHP or *o*-DHP. A movable hydride residing at the C2 position may explain why imidazolium species with Me substitutions at the C2 position do not appear to engage in CO_2 reduction catalysis.[11] This observation could be explained if the presence of the Me substituent at the C2 position kinetically prohibited the formation of a 4-imidazoline moiety on an electrode surface. Either hypothesis at this point can be considered as a possibility, although on the basis of energetics alone, a 0.2 V error in our calculations seems more realistic than 4-imidazoline forming at potentials employed in actual electrochemical cells.

In terms of electron substituent effects, adding electron-withdrawing or -donating groups to non-N-substituted imidazolium molecules influences hydricities and redox potentials qualitatively, as expected; however, we find that the degree of this effect is quantitatively less compared with similar substitutions on PyH^+ molecules. A deeper investigation of ANH substituents is currently underway in our group.

We now turn to N-Me-substituted imidazolium ANH molecules. Our investigations on 1,3-dimethyl-imidazolium molecules should be representative of EMIM molecules because the electronic structures and bonding nature of Me and Et substituents are similar. The fact that both N atoms have nonlabile substituents means that it will not readily donate or accept protons. The next most acidic site is the C2 atom, which has a pK_a of ~24 in water (Table 1). Thus, this ANH is unlikely to participate directly in proton shuttling. However, the $2e^-$ SRPs for these species are essentially the same as those for non-N-substituted imidazolium species. Again, it is possible that these SRPs are inaccurate by 0.2 V. As with the non-Me-substituted imidazolium molecules, if SRPs were calculated as 0.2 V more negative, then the same trends as found with pyridine would hold for these species. Again, it is also possible that the true species adsorbed on the electrode surface has a slightly more negative SRP than these reduced species in solution.

DOI: 10.1021/cs501406j
ACS Catal. 2015, 5, 1123−1130

Regardless, this ANH itself is unlikely to be capable of shuttling protons, so another Brønsted acid—namely, water—might enable protons to shuttle and react with CO_2. Again, Masel and co-workers used Ag electrodes rather than Pt, and Ag has a higher overpotential for HER. CO_2 reduction with Ag electrodes typically produces in CO + H_2O rather than formate. Furthermore, recent work by Masel has reported that increasing concentrations of water (which brings significant changes in the pH of the solution) had a significant impact on production of CO from CO_2.[14] Again, the presence of proton donors may help reduce these ANH molecules.

Finally, we also considered an ANH that is used in homogeneous photochemical conversion of CO_2 to methanol. Systems by MacDonnell and co-workers also include PyH^+ as a weak acid; however, within our hypothesis, PyH^+ would be able to convert to a DHP-like species only in the presence of an electrode with H_{opd}. Thus, these systems would likely require an efficient means of transferring multiple electrons, as well. As a first approximation to the full $[Ru(phen)_3]^{2+}$ chromophores, we calculated a Pourbaix diagram for an aqueous phase phenanthroline ligand. The Pourbaix diagram for this molecule is nearly identical to that for pyridine, even though the π system is substantially more extended. Our group is presently investigating how the presence of the metal center and other phenanthroline ligands would influence 1 and $2e^-$ SRPs as well as the Pourbaix diagrams for these complexes. In the meantime, thermodynamic energies presented by quantum chemistry indicates that the phenanthroline ligands on $[Ru(phen)_3]^{2+}$ themselves may play a similar noninnocent role facilitating hydride shuttling as Py.

In closing, MacDonnell and co-workers have also recently reported chromophores using internal pyridyl ligands that participate in photochemical CO_2 reduction in 1 M H_2O in DMF solution.[34] Here, photochemical experiments utilized the nonaqueous solvent because the chromophores otherwise have limited stability in water. A reaction mechanism was proposed that involved radical electrons forming on the pyridyl group before forming what was speculated to be a carbamate radical intermediate. This mechanism is essentially analogous to Bocarsly's original $PyH^+ + e^- \rightarrow PyH\cdot$ mechanism. Although the proposal of radicals forming on these larger ligands is certainly reasonable for photochemical processes, we previously ruled out radical carbamate formation because the barrier to form this intermediate in aqueous solution was found to have a high kinetic barrier ($\Delta H_{0,gas}^{\ddagger}$ = 25 kcal/mol, $\Delta G_{298,aq}^{\ddagger}$ = 32 kcal/mol).[22] We do not believe the barrier for forming similar carbamate radicals would be lower in this case. A more likely photochemical mechanism may be formation of a reduced ANH using steps analogous to those detailed by Musgrave et al.[29] Spectroscopic detection of this species in solution would help clarify this point.

CONCLUSIONS

We have carried out a first-principles quantum chemistry study of aromatic N-heterocycles (ANHs) that have been implicated in CO_2 electroreductions. We find convincing evidence that $2e^-$ SRPs for these molecules at pHs employed in experiments are quite similar to equilibrium redox potentials for CO_2 reduction products. Thus, under reduction conditions when protons or CO_2 would be reduced, it is also possible that the ANH molecules themselves may also become reduced and participate in this chemistry.

This finding has led us to propose some unifying explanations that may help guide future mechanistic proposals for other ANH-promoted CO_2 reductions as well as design principles for other renewable energy catalysts. Although the mechanisms for these processes remain unclear, there seems to be a correlation between multielectron SRPs and pK_as for ANH molecules present in solution and the pH and applied potentials employed where CO_2 reduction has been observed. We thus propose that computationally deriving Pourbaix diagram triple points can be a useful means to predict molecules that would facilitate efficient proton and electron transfers for the development of renewable energy catalysts. Further work in our group will investigate heterogeneous reaction mechanisms for ANH-promoted processes.

ASSOCIATED CONTENT

Supporting Information

The following file is available free of charge on the ACS Publications website at DOI: 10.1021/cs501406j.

Cartesian coordinates for optimized species and calculated free energies (PDF)

AUTHOR INFORMATION

Corresponding Author

*E-mail: jakeith@pitt.edu.

Notes

The authors declare no competing financial interest.

ACKNOWLEDGMENTS

We thank Profs. Kyle A. Grice, Michael J. Janik, and Eric J. Beckman for helpful discussions. We thank Jeffrey M. Carr for calculations of phenanthroline molecules. We also thank the Center for Simulation and Modeling at the University of Pittsburgh for technical support. This work was financially supported from startup funds from the Department of Chemical & Petroleum Engineering at the University of Pittsburgh and the R. K. Mellon Foundation.

REFERENCES

(1) Gust, D.; Moore, T. A.; Moore, A. L. *Acc. Chem. Res.* **2009**, *42*, 1890−1898.
(2) Gray, H. B. *Nat. Chem.* **2009**, *1*, 7.
(3) Fujita, E. *Coord. Chem. Rev.* **1999**, *185−186*, 373−384.
(4) Peterson, A. A.; Abild-Pedersen, F.; Studt, F.; Rossmeisl, J.; Norskov, J. K. *Energy Environ. Sci.* **2010**, *3*, 1311−1315.
(5) Mayer, J. M. *Annu. Rev. Phys. Chem.* **2004**, *55*, 363−390.
(6) Weinberg, D. R.; Gagliardi, C. J.; Hull, J. F.; Murphy, C. F.; Kent, C. A.; Westlake, B. C.; Paul, A.; Ess, D. H.; McCafferty, D. G.; Meyer, T. J. *Chem. Rev.* **2012**, *112*, 4016−4093.
(7) Hammes-Schiffer, S. *Acc. Chem. Res.* **2009**, *42*, 1881−1889.
(8) Barton Cole, E.; Lakkaraju, P. S.; Rampulla, D. M.; Morris, A. J.; Abelev, E.; Bocarsly, A. B. *J. Am. Chem. Soc.* **2010**, *132*, 11539−11551.
(9) Barton, E. E.; Rampulla, D. M.; Bocarsly, A. B. *J. Am. Chem. Soc.* **2008**, *130*, 6342−6344.
(10) Seshadri, G.; Lin, C.; Bocarsly, A. B. *J. Electroanal. Chem.* **1994**, *372*, 145−150.
(11) Bocarsly, A. B.; Gibson, Q. D.; Morris, A. J.; L'Esperance, R. P.; Detweiler, Z. M.; Lakkaraju, P. S.; Zeitler, E. L.; Shaw, T. W. *ACS Catal.* **2012**, *2*, 1684−1692.
(12) Rosen, B. A.; Haan, J. L.; Mukherjee, P.; Braunschweig, B.; Zhu, W.; Salehi-Khojin, A.; Dlott, D. D.; Masel, R. I. *J. Phys. Chem. C* **2012**, *116*, 15307−15312.

DOI: 10.1021/cs501406j
ACS Catal. 2015, 5, 1123−1130

(13) Rosen, B. A.; Salehi-Khojin, A.; Thorson, M. R.; Zhu, W.; Whipple, D. T.; Kenis, P. J. A.; Masel, R. I. *Science* **2011**, *334*, 643−644.
(14) Rosen, B. A.; Zhu, W.; Kaul, G.; Salehi-Khojin, A.; Masel, R. I. *J. Electrochem. Soc.* **2013**, *160*, H138−H141.
(15) Boston, D. J.; Xu, C.; Armstrong, D. W.; MacDonnell, F. M. *J. Am. Chem. Soc.* **2013**, *135*, 16252−16255.
(16) Xiang, D.; Magana, D.; Dyer, R. B. *J. Am. Chem. Soc.* **2014**, *136*, 14007−14010.
(17) Bara, J. E.; Camper, D. E.; Gin, D. L.; Noble, R. D. *Acc. Chem. Res.* **2010**, *43*, 152−159.
(18) Bates, E. D.; Mayton, R. D.; Ntai, I.; Davis, J. H. *J. Am. Chem. Soc.* **2002**, *124*, 926−927.
(19) Ertem, M. Z.; Konezny, S. J.; Araujo, C. M.; Batista, V. S. *J. Phys. Chem. Lett.* **2013**, *4*, 745−748.
(20) Keith, J. A.; Carter, E. A. *J. Am. Chem. Soc.* **2012**, *134*, 7580−7583.
(21) Keith, J. A.; Carter, E. A. *J. Chem. Theory Comput.* **2012**, *8*, 3187−3206.
(22) Keith, J. A.; Carter, E. A. *Chem. Sci.* **2013**, *4*, 1490−1496.
(23) Keith, J. A.; Carter, E. A. *J. Phys. Chem. Lett.* **2013**, *4*, 4058−4063.
(24) Lim, C. H.; Holder, A. M.; Musgrave, C. B. *J. Am. Chem. Soc.* **2013**, *135*, 142−154.
(25) Costentin, C.; Canales, J. C.; Haddou, B.; Savéant, J.-M. *J. Am. Chem. Soc.* **2013**, *135*, 17671−17674.
(26) Lebègue, E.; Agullo, J.; Morin, M.; Bélanger, D. *ChemElectroChem.* **2014**, *1*, 1013−1017.
(27) Yan, Y.; Zeitler, E. L.; Gu, J.; Hu, Y.; Bocarsly, A. B. *J. Am. Chem. Soc.* **2013**, *135*, 14020−14023.
(28) Tossell, J. A. *Comp. Theor. Chem.* **2011**, *977*, 123−127.
(29) Lim, C. H.; Holder, A. M.; Hynes, J. T.; Musgrave, C. B. *J. Am. Chem. Soc.* **2014**, *136*, 16081−16095.
(30) Riboni, F.; Selli, E.; Hoffmann, M. R.; Colussi, A. J. *J. Phys. Chem. A* **2014**, *118*, 10.1021/jp509735z.
(31) Jerkiewicz, G. *Electrocatal.* **2010**, *1*, 179−199.
(32) Conway, B. E.; Bai, L. *J. Chem. Soc., Faraday Trans. 1* **1985**, *81*, 1841−1862.
(33) Portenkirchner, E.; Enengl, C.; Enengl, S.; Hinterberger, G.; Schlager, S.; Apaydin, D.; Neugebauer, H.; Knör, G.; Sariciftci, N. S. *ChemElectroChem.* **2014**, *1*, 1013−1017.
(34) Boston, D. J.; Pachón, Y. M. F.; Lezna, R. O.; de Tacconi, N. R.; MacDonnell, F. M. *Inorg. Chem.* **2014**, *53*, 6544−6553.
(35) McSkimming, A.; Colbran, S. B. *Chem. Soc. Rev.* **2013**, *42*, 5439−5488.
(36) Schmidt, M. W.; Baldridge, K. K.; Boatz, J. A.; Elbert, S. T.; Gordon, M. S.; Jensen, J. H.; Koseki, S.; Matsunaga, N.; Nguyen, K. A.; Su, S.; Windus, T. L.; Dupuis, M.; Montgomery, J. A. *J. Comput. Chem.* **1993**, *14*, 1347−1363.
(37) Piera, J.; Bäckvall, J.-E. *Angew. Chem., Int. Ed.* **2008**, *47*, 3506−3523.
(38) Becke, A. D. *Phys. Rev. A* **1988**, *38*, 3098−3100.
(39) Lee, C.; Yang, W.; Parr, R. G. *Phys. Rev. B* **1988**, *37*, 785−789.
(40) Dunning, T. H. *J. Chem. Phys.* **1989**, *90*, 1007−1023.
(41) Barone, V.; Cossi, M. *J. Phys. Chem. A* **1998**, *102*, 1995−2001.
(42) Knizia, G.; Adler, T. B.; Werner, H.-J. *J. Chem. Phys.* **2009**, *130*, 054104.
(43) Weigend, F. *Phys. Chem. Chem. Phys.* **2002**, *4*, 4285−4291.
(44) Weigend, F.; Köhn, A.; Hättig, C. *J. Chem. Phys.* **2002**, *116*, 3175−3183.
(45) Yousaf, K. E.; Peterson, K. A. *Chem. Phys. Lett.* **2009**, *476*, 303−307.
(46) Werner, H.-J.; P. J. K, Knizia, G.; Manby, F. R.; M. Schütz, Celani, P.; Korona, T.; Lindh, R.; Mitrushenkov, A.; Rauhut, G.; K. Shamasundar, R.; Adler, T. B.; Amos, R. D.; Bernhardsson, A.; Berning, A.; Cooper, D. L.; Deegan, M. J. O.; Dobbyn, A. J.; Eckert, F.; Goll, E.; Hampel, C.; Hesselmann, A.; Hetzer, G.; Hrenar, T.; Jansen, G.; C. Köppl, Liu, Y.; Lloyd, A. W.; Mata, R. A.; May, A. J.; McNicholas, S. J.; Meyer, W.; Mura, M. E.; Nicklaß, A.; D. P. O'Neill, Palmieri, P.; Peng, D.; K. Pflüger, Pitzer, R.; Reiher, M.; Shiozaki, T.; Stoll, H.; Stone, A. J.; Tarroni, R.; Thorsteinsson, T.; Wang, M. *MOLPRO*, version 2010.1, a package of ab initio programs, 2008; Cardiff University: Cardiff, United Kingdom.
(47) Ho, J.; Coote, M. L. *Theor. Chem. Acc.* **2009**, *125*, 3−21.
(48) Creutz, C.; Chou, M. H.; Hou, H.; Muckerman, J. T. *Inorg. Chem.* **2010**, *49*, 9809−9822.
(49) Baik, M.-H.; Friesner, R. A. *J. Phys. Chem. A* **2002**, *106*, 7407−7412.
(50) McQuarrie, D. A. *Statistical Mechanics*. 1st ed.; University Science Books: Sausalito, 2000; p 86.
(51) Tissandier, M. D.; Cowen, K. A.; Feng, W. Y.; Gundlach, E.; Cohen, M. H.; Earhart, A. D.; Coe, J. V.; Tuttle, T. R. *J. Phys. Chem. A* **1998**, *102*, 7787−7794.
(52) Isse, A. A.; Gennaro, A. *J. Phys. Chem. B* **2010**, *114*, 7894−7899.
(53) Marenich, A. V.; Ho, J.; Coote, M. L.; Cramer, C. J.; Truhlar, D. G. *Phys. Chem. Chem. Phys.* **2014**, *16*, 15068−15106.
(54) Creutz, C.; Chou, M. H. *J. Am. Chem. Soc.* **2009**, *131*, 2794−2795.
(55) Greeley, J.; Jaramillo, T. F.; Bonde, J.; Chorkendorff, I. B.; Nørskov, J. K. *Nat. Mater.* **2006**, *5*, 909−913.
(56) Greeley, J.; Stephens, I. E.; Bondarenko, A. S.; Johansson, T. P.; Hansen, H. A.; Jaramillo, T. F.; Rossmeisl, J.; Chorkendorff, I.; Nørskov, J. K. *Nat. Chem.* **2009**, *1*, 552−556.
(57) Man, I. C.; Su, H.-Y.; Calle-Vallejo, F.; Hansen, H. A.; Martínez, J. I.; Inoglu, N. G.; Kitchin, J.; Jaramillo, T. F.; Nørskov, J. K.; Rossmeisl, J. *ChemCatChem.* **2011**, *3*, 1159−1165.
(58) Peterson, A. A.; Nørskov, J. K. *J. Phys. Chem. Lett.* **2012**, *3*, 251−258.
(59) Barton Cole, E. *Pyridinium-Catalyzed Electrochemical and Photoelectrochemical Conversion of CO_2 to Fuels*; Princeton University: Princeton, NJ, 2009.
(60) Dissociation Constants of Organic Acids and Bases. In *CRC Handbook of Chemistry and Physics*; Haynes, W. M., Ed.; CRC Press/Taylor and Francis: Boca Raton, 2014; pp 5−96.
(61) Electrolytes, Electromotive Force, and Chemical Equilibrium. In *Lange's Handbook of Chemistry*, 15th ed.; Dean, J. A., Ed.; McGraw-Hill Inc.: New York, 1999; pp 8−37.
(62) Bruehlmann, U.; Hayon, E. *J. Am. Chem. Soc.* **1974**, *96*, 6169−6175.
(63) Walba, H.; Isensee, R. W. *J. Org. Chem.* **1961**, *26*, 2789−2791.
(64) Amyes, T. L.; Diver, S. T.; Richard, J. P.; Rivas, F. M.; Toth, K. *J. Am. Chem. Soc.* **2004**, *126*, 4366−4374.
(65) Irving, H.; Mellor, D. H. *J. Chem. Soc.* **1962**, 5222−5237.

DOI: 10.1021/cs501406j
ACS Catal. 2015, 5, 1123−1130